

A Cross-Layer Design Perspective for Multi-Resolution Signaling

A. Annamalai and Jia Liu
 Mobile and Portable Radio Research Group
 Virginia Tech
 432 Durham Hall (0350), Blacksburg, VA 24061
 Email: {kevinlau, annamalai}@vt.edu

Abstract—In this article, we analyze the performance of two selective repeat automatic repeat request (SR-ARQ) schemes, which exploit the differences in bit protection levels of M-ary PSK symbols (with Gray code mapping), to support multimedia multicasting in wireless networks. Our simulation results reveal that the throughput performance of the proposed SR-ARQ schemes are significantly better than the traditional SR-ARQ scheme in a myriad of fading environments. The relative throughput improvement is greater for channels that experience severe deep fades and fast fading at moderate and large mean SNR/symbol values. However, the power efficiency improvement appears to be relatively insensitive to both fade distribution and user mobility.

I. INTRODUCTION

Digital modulation techniques that employ nonuniform signal constellation [1], [2] have recently received considerable interest for multicasting multimedia messages to receivers of different capabilities [3]–[5] and for broadcasting digital data and video signal [6]. Previous studies have primarily focused on the multicast signal design [3]–[5] and the computation of bit error rate for generalized QAM and PSK hierarchical constellations [7], [8], although the potential benefits of multi-resolution signalling cannot be fully realized without close interactions between the physical layer and upper layers in the protocol stack. In [9], we show that the benefits of multi-resolution signaling can be further leveraged at the data link layer (by introducing a slight modification to the conventional selective-repeat ARQ protocol) for improving the data throughput without any instantaneous feedback of channel quality measurements, without altering the signal constellation at the transmitter, and without using error control coding with incremental redundancy.

In this article, we extend our previous work on the joint design of physical/data link layers for multi-resolution signaling by considering the effects of fade distribution, correlations between fading symbols (i.e., Doppler frequency) and disparity between quality of service (QoS) requirements for different classes of bits (in an M-ary symbol) on the normalized throughput and power efficiency performance metrics.

II. SYSTEMS MODEL

A. Nonuniform M-PSK Constellation

Consider a nonuniform 8-PSK constellation as depicted in Fig. 1. The actual symbols are represented by small circles

and Gray labelled. The first level and the second level virtual symbol points in Fig. 1 are represented by “×” and “+” respectively. The phase offset angles for our nonuniform M-PSK constellation θ_i ($i = 1, 2, \dots, m - 1$) is given by

$$\theta_i = \frac{\pi}{2} \beta^i, \quad i = 1, 2, \dots, m - 1. \quad (1)$$

The reason for fixing the ratio of the angles for any subsequent levels of signal constellation hierarchy β to a constant is to facilitate the phase offset optimization (i.e., only a single design parameter needs to be optimized as required in [3]–[5] rather than manipulating $m - 1$ variables). Also notice that when $\beta = 0.5$, the system reverts to a uniform 8-PSK signal constellation.

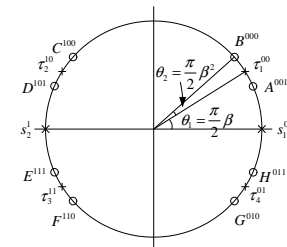


Fig. 1. Nonuniform 8-PSK constellation.

B. Modified SR-ARQ Protocols

Suppose we want to support multimedia data transmission (i.e., three traffic bit streams with distinct BER requirements) in a point-to-point communication. In the conventional (baseline) 8-PSK modulation scheme, the required SNR per bit γ_{req} must be chosen to satisfy the most stringent QoS requirement. The symbols (each consisting of three bits in this example)

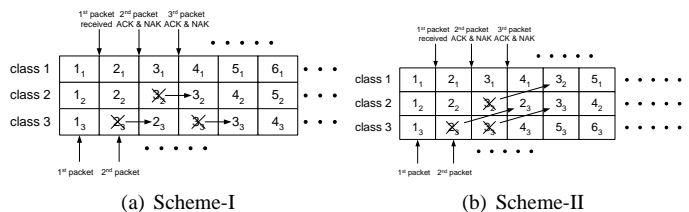


Fig. 2. Operations of SR-ARQ Scheme-I and II.

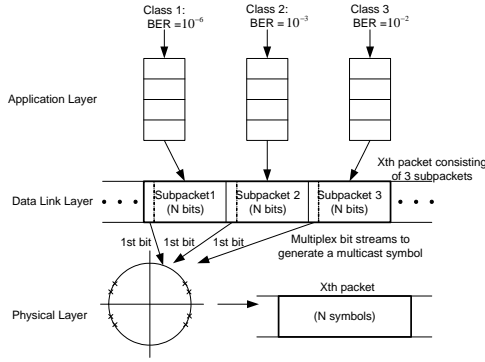


Fig. 3. System Operation.

will be transmitted over the physical communication channel. Hence, the required SNR/symbol is $3\gamma_{req}$.

Now, consider two variants of SR-ARQ protocol (SR-ARQ Scheme-I and SR-ARQ Scheme-II) depicted in Fig. 2(a) and Fig. 2(b). The operation of the whole system is depicted in Fig. 3. In our modified SR-ARQ schemes, the N multicast 8-PSK symbols received from the X^{th} packet are first demultiplexed into three subpackets corresponding to the three different traffic classes (each subpacket consists of N bits). Note that the data bits from the traffic class which requires the most error protection (i.e., highest γ_{req}) will be assigned to the most significant bit of each multicast symbol at the transmitter while the least significant bit of each multicast symbol corresponds to the bits from the traffic class with the smallest γ_{req} .

In SR-ARQ Scheme-I, the subpackets that were received in error will be retransmitted using the same error protection level. In SR-ARQ Scheme-II, the negative acknowledged (NAK) subpacket will be retransmitted with better error protection (if possible). It should be apparent by now that the link layer in our modified SR-ARQ schemes may be able to recover a fraction of the erroneous packet successfully (i.e., even though a symbol is received in error, some of the bits of that symbol may be received correctly due to the inherent better error protection for the higher significant bits in the multicast constellation). This benefit cannot be realized in the conventional SR-ARQ scheme because no attempt is made to exploit the differences in the bit error protection among the bits in an M-ary signal constellation.

In [9] we have derived the normalized throughput expressions for subpacket class i with nonuniform 8-PSK modulation for both SR-ARQ Scheme-I and SR-ARQ Scheme-II. The normalized throughput of subpacket class 1, 2 and 3 for SR-ARQ Scheme-I, denoted by $S_1^{(1)}$, $S_2^{(1)}$, and $S_3^{(1)}$ respectively, are summarized below:

$$S_i^{(1)} = 1 - P_{spi}, \quad i = 1, 2, 3 \quad (2)$$

where P_{spi} corresponds to the subpacket error rate for traffic class i . The normalized throughput for the different classes of

traffic in SR-ARQ Scheme-II are given by:

$$S_1^{(2)} = 1 - P_{sp1} \quad (3)$$

$$S_2^{(2)} = \frac{1 - P_{sp1}}{1 - P_{sp1} + P_{sp2}} \quad (4)$$

$$S_3^{(2)} = \frac{1 - P_{sp1}}{(1 - P_{sp1})(1 + P_{sp3}) + P_{sp2}P_{sp3}} \quad (5)$$

Then the normalized average throughput is calculated as

$$\eta = \frac{1}{3} \sum_{i=1}^3 S_i^{(k)}, \quad k = 1, 2. \quad (6)$$

III. SIMULATION RESULTS AND DISCUSSIONS

A. Fading Channel Simulator

In this article, we developed an accurate composite fading channel simulator that captures both the log-normal shadowing and the Rice multipath fading processes. The random fading envelopes are produced by first generating complex Gaussian random variables in the frequency domain and then shaping the random signals in one of the two arms using the spectral filter derived by (7) while shaping the random signals on the other arm using (8). Finally, accurate time-domain samples of the Doppler fading are generated by performing inverse fast Fourier transform (IFFT) operations at each arm and then adding both the fading samples together. The Doppler frequency spectrum of Rice multipath fading channel model is given by

$$S_{\text{Rice}}(f) = \frac{1.5}{\pi f_m \sqrt{1 - \left(\frac{f-f_c}{f_m}\right)^2}} + \frac{3K}{K+1} \delta(f - f_m \cos \alpha) \quad (7)$$

where K is the Rice factor, f_c denotes the carrier frequency, f_m corresponds to the maximum doppler frequency shift, and α is the angle of incidence.

In addition to the short-term Rice fading, there is also slower variation of the short-term mean strength of the received signal. This phenomenon is referred to as shadowing, which is often observed to be log-normally distributed, but its autocorrelation function is generally unknown and heavily depends on the distribution of terrain features. In our simulation, we have considered (8) as a representative of the frequency spectrum for the log-normal fading process:

$$S_{\text{log-normal}}(f) = \frac{1}{0.0101 \cdot f_m \cdot \frac{c}{f_c} + j2\pi f} \quad (8)$$

Note that (8) is derived by evaluating the Fourier transform of the autocorrelation function defined by Eq. (2) in [10] (which is obtained from experimental data with continuous wave at 842MHz in the Osaka metropolitan area). Fig. 4 illustrate the time sequence generated by our fading simulator.

B. Computational and Simulation Results

Let $\gamma_{req}^{(i)}$ denote the required SNR/bit for a specified QoS requirement for class i traffic. The simulation curves for the normalized average throughput were obtained using 10,000

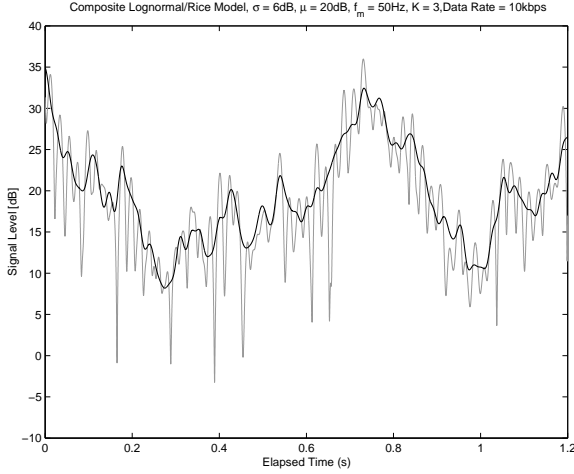


Fig. 4. Composite log-normal shadowing and Rice fading channel.

packets in Rice fading or composite log-normal and Rice fading channel models. A subpacket is considered error free if all the N bits are received correctly (i.e., SNR/bit of the N fading samples in the subpacket is above $\gamma_{req}^{(i)}$). Suppose that the length of each subpacket is $N = 128$. If at least one out of N bits is below $\gamma_{req}^{(i)}$, then the subpacket must be retransmitted. Therefore, the subpacket error rate is given by

$$P_{spi} = \Pr \left\{ \frac{\text{Symbols in a subpacket above } \gamma_{req}^{(i)}}{N} < 1 \right\} \quad (9)$$

To determine $\gamma_{req}^{(i)}$, we need to invert the exact bit error rate expressions for the multicast constellations, which can be very cumbersome since no closed-form solutions exist. This task can be greatly simplified by approximating the exact bit error rate as

$$P_{e,\beta}^{(i)} = a_{\beta}^{(i)} e^{-b_{\beta}^{(i)} \gamma^{(i)}} + c_{\beta}^{(i)} e^{-2b_{\beta}^{(i)} \gamma^{(i)}}. \quad (10)$$

In (10), $a_{\beta}^{(i)}$, $b_{\beta}^{(i)}$, and $c_{\beta}^{(i)}$ are assumed to be a 3rd order polynomial in the form of

$$p_1 \beta^3 + p_2 \beta^2 + p_3 \beta + p_4, \quad (11)$$

where p_1 , p_2 , p_3 , and p_4 are constants which are tabulated in Table I in [9] for a nonuniform 8-PSK modulation. For instance, consider three classes of traffic with BER requirements 10^{-6} , 10^{-3} , and 10^{-2} . The required SNR/bit for different traffic classes as a function of the phase offset ratio β are plotted in Fig. 5. This figure also illustrates the usefulness of the approximate BER expressions derived in [9].

In Fig. 6, the normalized average throughput for both the SR-ARQ (uniform 8-PSK) and the modified SR-ARQ schemes (multicast 8-PSK with optimized $\beta = 0.428$, $\gamma_{req}^{(1)} = 15.096$, $\gamma_{req}^{(2)} = 14.688$, $\gamma_{req}^{(3)} = 15.263$) are plotted as a function of the long-term mean channel SNR/symbol. It is assumed that the carrier frequency is 800MHz and user velocity is 40km/hour. We observe that the power efficiency improvement (using modified SR-ARQ protocols in conjunction with the optimized 8-PSK multicast constellation) is more than 5dB for

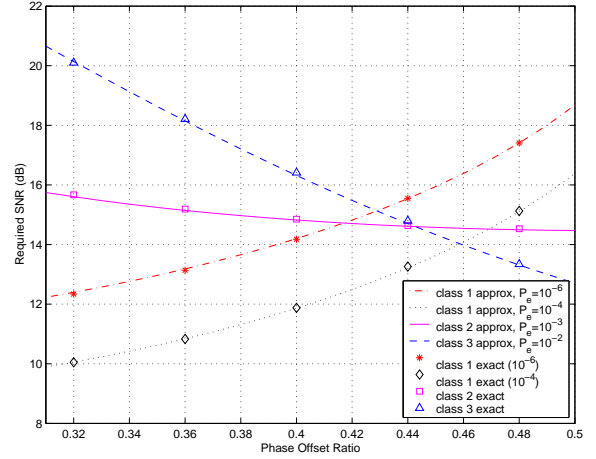


Fig. 5. Required SNR/bit for different classes of services.

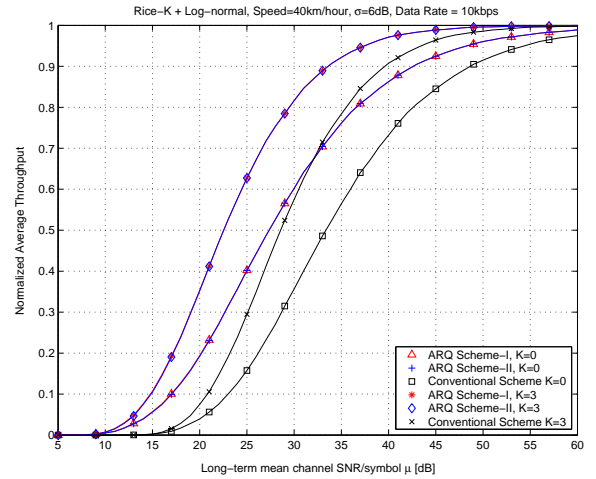


Fig. 6. The normalized throughput in composite log-normal and Rice fading environments.

both Suzuki (shadowed Rayleigh) and shadowed Rice fading channels. The relative throughput improvement is greater when the channel experience more severe fading.

In Fig. 7, the normalized average throughput for different SR-ARQ protocols are plotted over Rice and Rayleigh ($K=0$) fading channels. The trends of the performance curves are similar to that observed from Fig. 6. The difference in the short-term average channel SNR/symbol between the conventional SR-ARQ and the modified SR-ARQ schemes is approximately 6dB.

In Fig. 8, we investigate the effect of mobile velocity (i.e., Doppler rate) on the performance of various SR-ARQ protocols. The normalized average throughput is lower for the fast fading case compared to the slow fading scenario as expected. Although the relative throughput improvement is generally greater at higher mobile velocity, the difference in the average SNR/symbol between the conventional SR-ARQ and the SR-ARQ Scheme-I (or the SR-ARQ Scheme-II) at a specified normalized average throughput appears to be insensitive to the change in the Doppler frequency.

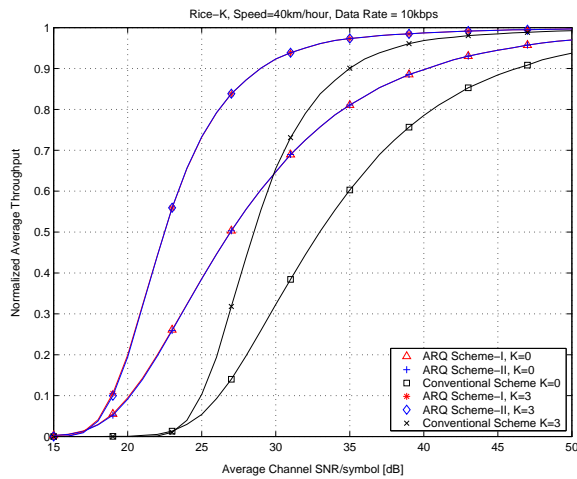


Fig. 7. The normalized average throughput in Rice and Rayleigh fading environments.

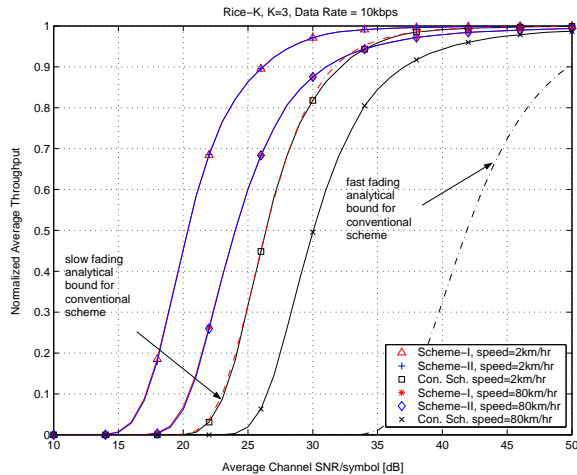


Fig. 8. Effect of mobile velocity on the normalized average throughput in a Rice fading channel.

To further validate the trends in our simulation results that takes into account of the fading symbol correlations, we may derive an analytical bound for the subpacket error rate as follows:

$$F_\gamma(\gamma_{req}) \leq P_{spi} \leq 1 - (1 - F_\gamma(\gamma_{req}))^N. \quad (12)$$

where $F_\gamma(x)$ denotes the cumulative distribution function (CDF) of the channel SNR evaluated at x . The lower bound for the subpacket error rate corresponds to a very slow fading scenario (i.e., the entire subpacket experience identical fading), while its upper bound corresponds to a very fast fading scenario (i.e., each bit of the subpacket experience independent fading).

Similarly, for the conventional SR-ARQ scheme, the packet error rate P_E is bounded by

$$F_\gamma(\gamma_{th}) \leq P_E \leq 1 - (1 - F_\gamma(\gamma_{th}))^N, \quad (13)$$

where $\gamma_{th} = 3\gamma_{req}$ and γ_{req} corresponds to the SNR/bit that satisfies the most stringent QoS requirement (obtained from

the average BER curve for the 8-PSK).

For example, the CDF $F_\gamma(x)$ for the Rice fading channel is given by

$$F_\gamma(x) = 1 - Q \left[\sqrt{2K}, \sqrt{\frac{2(1+K)x}{\Omega}} \right] \quad (14)$$

where the Marcum Q-function is defined by $Q(\sqrt{2a}, \sqrt{2b}) = \int_b^\infty e^{-(t-a)} I_0(2\sqrt{at}) dt$, and K denotes the Rice factor.

The analytical bounds for the normalized average throughput of the conventional SR-ARQ is also plotted in Fig. 8 by setting $\gamma_{req} = 21.045\text{dB}$.

IV. CROSS-LAYER OPTIMIZATION FOR MULTI-RESOLUTION SIGNALING

Since battery-life is limited, power efficiency is an important design consideration for mobile terminals. Our results and discussions in Section III reveal that nonuniform signal constellations can be used to facilitate multimedia traffic with lower power consumption, or yield higher throughput, or extend the communication range.

To systematically determine the optimal phase offset ratio β which satisfy the requirements for all distinct classes of bit stream while ensuring the fairness among them in a point-to-point communication, we may employ the following optimization algorithm:

$$\begin{aligned} & \arg \min_{\beta} \left\{ \max_i \left\{ \gamma_{req}^{(i)} \right\} \right\} \\ \text{s.t. } & P_b^{(1)} \leq 10^{-4} \\ & P_b^{(2)} \leq 10^{-3} \\ & P_b^{(3)} \leq 10^{-2} \\ & \beta \in (0, 0.5], i \in \{1, 2, 3\} \end{aligned} \quad (15)$$

Solving (15) with the aid of the approximate closed-form BER formulas derived in [9], we found that the optimal (i.e., the most power-efficient) β is 0.47 ($\gamma_{req}^{(1)} = 14.6\text{dB}$, $\gamma_{req}^{(2)} = 14.5\text{dB}$, $\gamma_{req}^{(3)} = 13.7\text{dB}$). This result may be also deduced graphically from Fig. 5. Thus our algorithm facilitates the task of phase offset ratio optimization in real-time. It is also important to note that with this choice of β , the difference in normalized average throughput between Scheme-I and Scheme-II will be negligible.

We also found that the efficacy of nonuniform signal constellation as the disparity between QoS requirements for different classes of bits vanishes. For example, the power efficiency improvement is reduced to about 2.3dB from approximately 5dB when the BER requirement for classes 1 is altered from 10^{-6} to 10^{-4} .

In Fig. 9 and Fig. 10, we investigate the efficacy of SR-ARQ Scheme-II to maximize the normalized average throughput of multimedia traffic in Rayleigh and Rice fading channels respectively, at two different link qualities (mean SNR/symbol). It was observed that the necessary condition for SR-ARQ Scheme-II to outperform Scheme-I is given by

$$\gamma_{req}^{(1)} \leq \gamma_{req}^{(2)} \leq \gamma_{req}^{(3)}. \quad (16)$$

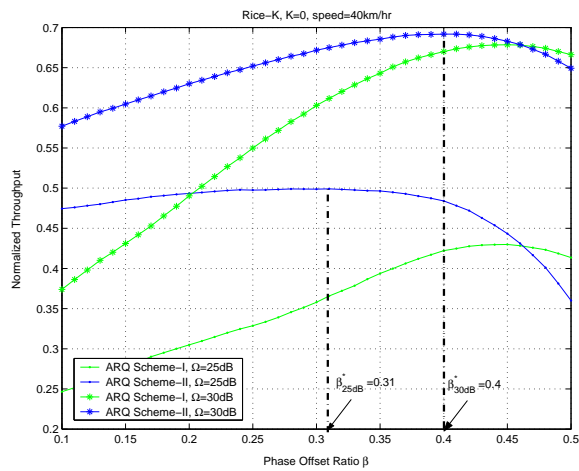


Fig. 9. Normalized throughput versus β in Rayleigh fading (BER requirement of 10^{-4} , 10^{-3} , and 10^{-2}).

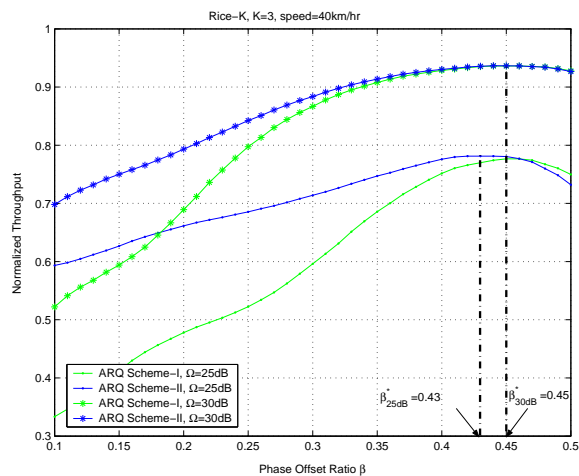


Fig. 10. Normalized average throughput versus β in Rice fading (BER requirements of 10^{-4} , 10^{-3} , and 10^{-2}).

Fig. 9 also reveals that a different criterion (maximizing normalized average throughput) may be used for optimizing β in conjunction with SR-ARQ Scheme-II. This benefit, however, vanishes when the channel experiences fewer deep fades and at higher channel SNR/symbol.

In a practical mobile ad hoc network, the channels between the nodes may differ considerably because of the differences in propagation characteristics, interference levels and due to the differing capabilities of the heterogeneous nodes themselves. Thus, the selection of optimal β for multimedia multicasting must also consider the different link qualities of the nodes in the receiving cluster as discussed in [9].

Another application of the multi-resolution signaling is that we can multiplex traffics of different users (each user has different link qualities and different QoS requirements) to nonuniform constellations. Suppose that there are three users A , B , and C with average channel SNR 35dB, 45dB, and 25dB

respectively, and the according BER requirements are 10^{-6} , 10^{-3} , and 10^{-2} . Therefore, the traffic of A , B , and C can be

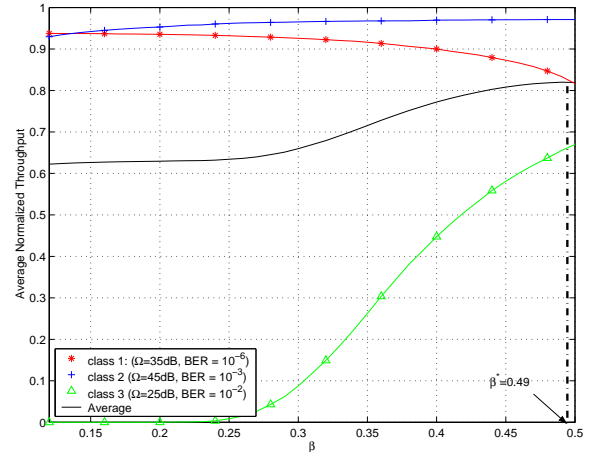


Fig. 11. Average throughput of multiplexing different users with different channel link qualities and QoS requirements to nonuniform constellations.

transmitted by class 1, 2, and 3 respectively. Suppose that the Rice factor $K = 3$, data rate is 10kbps, and mobile velocity is 40km/hour. The average normalized throughput of Scheme-I is plotted in Fig. 11. To maximize the average throughput of three users, it is seen from Fig. 11 that the optimal β is 0.49. This application is particularly useful to combat the near-far problem in CDMA forward link.

REFERENCES

- [1] M. Morimoto, H. Harada, M. Okada, and S. Komaki, "A study on power assignment of hierarchical modulation schemes for digital broadcasting," *IEICE Trans. Commun.*, vol. E77-B, Dec. 1994.
- [2] M. Sajadieh, F. Kschischang and A. Leon-Garcia, "Modulation-Assisted Unequal Error Protection over the Fading Channel," *IEEE Trans. Vehic. Technol.*, vol. 47, pp. 900-908, Aug. 1998
- [3] M. Pursley and J. Shea, "Nonuniform phase-shift-key modulation for multimedia multicast transmission in mobile wireless networks," *IEEE J. Select Areas Commun.*, vol. 17, No. 5, pp. 773-783, May 1999.
- [4] M. Pursley and J. Shea, "Multimedia multicast wireless communications with phase-shift-key modulation and convolutional coding," *IEEE J. Select Areas Commun.*, vol. 17, No. 11, pp. 1999 - 2010, Nov. 1999.
- [5] M. Pursley and J. Shea, "Adaptive nonuniform phase-shift-key modulation for multimedia traffic in wireless networks," *IEEE J. Select Areas Commun.*, vol. 18, No. 8, pp. 1394-1407, Aug. 2000.
- [6] DVB-T standard: ETS 300 744, Digital broadcasting systems for television, sound and data services; framing structure, channel coding and modulation for digital terrestrial television, ETSI Draft, vol. 1.2.1, no. EN300 744, 1999
- [7] P. Vittahaladevuni and M. S. Alouini, "A recursive algorithm for the exact BER computation of generalized hierarchical QAM constellations," *IEEE Trans. Info. Theory*, vol. 49, pp. 297 - 307, Jan. 2003.
- [8] P. Vittahaladevuni and M. Alouini, "Exact BER computation of generalized hierarchical PSK constellations," *IEEE Trans. Commun.*, vol. 51, pp. 2030-2037, Dec. 2003.
- [9] J. Liu and A. Annamalai, "Multi-Resolution Signaling for Multimedia Multicasting," to appear in *Proc. IEEE VTC Fall, 2004*.
- [10] S. Hara, A. Ogino, M. Araki, M. Okada, and N. Morigana, "Throughput Performance of SAW-ARQ Protocol with Adaptive Packet Length in Mobile Packet Data Transmission," *IEEE Trans. of Vehicular Technology*, vol. 45, pp. 561 - 569, Aug. 1996.